Comprehensive *in silico* and functional studies for classification of *EPAS1/HIF2A* genetic variants identified in patients with erythrocytosis

Valéna Karaghiannis,[1,2*] Darko Maric,[3,4*] Céline Garrec,[5] Nada Maaziz,[6] Alexandre Buffet,[7,8] Loïc Schmitt,[2] Vincent Antunes,[3,4] Fabrice Airaud,[5] Bernard Aral,[6] Amandine Le Roy,[2] Sébastien Corbineau,[2] Lamisse Mansour-Hendili,[9,10] Valentine Lesieur,[2] Antoine Rimbert,[2] Fabien Laporte,[2] Marine Delamare,[2] Minke Rab,[11,12] Stéphane Bézieau,[2,5] Bruno Cassinat,[13] Frédéric Galacteros,[10,14] Anne-Paule Gimenez-Roqueplo,[7,8] Nelly Burnichon,[7,8] Holger Cario,[15] Richard van Wijk,[11] Celeste Bento,[16] ECYT-4 consortium,° François Girodon,[6,17,18#] David Hoogewijs,[3,4#] and Betty Gardie[1,2,18#]

[1]Ecole Pratique des Hautes Etudes, EPHE, Université Paris Sciences et Lettres, Paris, France; [2]Nantes Université, CNRS, INSERM, l'Institut du Thorax, Nantes, France; [3]Section of Medicine, Department of Endocrinology, Metabolism and Cardiovascular System, University of Fribourg, Fribourg, Switzerland; [4]National Center of Competence in Research "Kidney.CH", Switzerland; [5]Service de Génétique Médicale, CHU de Nantes, Nantes, France; [6]Service d'Hématologie Biologique, Pôle Biologie, CHU de Dijon, Dijon, France; [7]Université Paris Cité, INSERM, PARCC, Paris, France; [8]Département de Médecine Génomique des Tumeurs et des Cancers, AP-HP, Hôpital Européen Georges Pompidou, Paris, France; [9]Département de Biochimie-Biologie Moléculaire, Pharmacologie, Génétique Médicale, AP-HP, Hôpitaux Universitaires Henri Mondor, Créteil, France; [10]Université Paris-Est Créteil, IMRB Equipe Pirenne, Laboratoire d'Excellence LABEX GRex, Créteil, France; [11]Central Diagnostic Laboratory - Research, University Medical Center Utrecht, Utrecht University, Utrecht, the Netherlands; [12]Department of Hematology, University Medical Center Utrecht, Utrecht University, Utrecht, the Netherlands; [13]Université Paris Cité, APHP, Hôpital Saint-Louis, Laboratoire de Biologie Cellulaire, Paris, France; [14]Red Cell Disease Referral Center-UMGGR, AP-HP, Hôpitaux Universitaires Henri Mondor, Créteil, France; [15]Department of Pediatrics and Adolescent Medicine, University Medical Center, Ulm, Germany; [16]Hematology Department, Centro Hospitalar e Universitário de Coimbra, CIAS, University of Coimbra, Coimbra, Portugal; [17]Université de Bourgogne, INSERM U1231, Dijon, France and [18]Laboratoire d'Excellence GR-Ex, Paris, France

[*]VK and DM contributed equally as co-first authors.
[#]FG, DH and BG contributed equally as co-senior authors.
°An appendix with all ECYT-4 consortium members can be found at the end of the manuscript.

Correspondence: B. Gardie
betty.gardie@inserm.fr

Received: September 1, 2022.
Accepted: January 17, 2023.
Early view: January 26, 2023.

https://doi.org/10.3324/haematol.2022.281698

Supplementary Data

Methods

Sequencing

Series of patients presenting with erythrocytosis were collected for sequencing in laboratories of genetic diagnosis : 450 patients in Nantes and Dijon (France), 280 patients in Créteil (Mondor), France ; 90 in St Louis Hospital, France; 160 patients in Ulm, Germany; 250 patients in Netherland, 220 patients in Coimbra, Portugal. DNA was extracted from whole blood on EDTA by using the QuickGene DNA Whole blood kit L (Kurabo) on the QuickGene610L® (in Nantes), QIAGEN spin-columns on the QIAcube (St Louis Hospital, France), silica matrix columns from QIAGEN (Hilden, Germany) (in Ulm, Germany), QIAGEN gDNA Blood Kit on the QIAsymphony SP (Coimbra, Portugal).

Molecular screening was performed by high throughput sequencing with different technologies, depending on the sequencing center: KAPA HyperPlus" (Roche) associated with IDT probes for the capture provided by Sophia Genetics (Nantes and Dijon, France), KAPA Hyperchoice Max 3MB T3 - 12 RXN (Roche) (Créteil, France), HaloPlex (Agilent) with sequencing on MiSeq and bioinformatic analysis with SureSelect (St Louis Hospital, France), Agilent SureSelectXT capture library and sequence analysis on the Illumina sequencing platform (Netherland), AmpliSeq Library with sequencing on Plataforma IonS5 (Thermo Fisher Scientific) (Coimbra, Portugal). The NGS panel contained the following genes: *VHL, EGLN1, EGLN2, EGLN3, HIF1A, EPAS1, EPO-R, SH2B3, JAK2, BPGM*, *EPO* (Nantes and Dijon, France), *BPGM, CYB5R3, EGLN1, EGLN2, EGLN3, HIF2A, HIF1A, HIF1AN, HIF3A, EPO, EPOR, SH2B3, VHL, JAK2, HBB, HBA1, HBA2 , MPL, CALR , KDM6A, GFI1B, BHLHE41, OS9, ZNF197, PIEZO1, MVK , THRA, FH, HIKESHI, HSF1, HSPA4, HSPA8, HSPB1, HSPH1, MITF, P4HTM, USP20, VHLL, XPO1* (Créteil, France), *BPGM, EGLN1, EGLN2, EGLN3, EPAS1, EPO, EPOR, FH, HIF1A, HIF1AN, HIF3A, JAK2, MITF, P4HTM, SH2B3, USP20, VHL, VHLL, GFI1B* (St Louis Hospital, France), *BPGM*, *EGLN1*, *EGLN2*, *EGLN3*, *EPAS1*, *EPO*, *EPOR*, *HBA1*, *HBA2*, *HBB*, *HIF1A*, *HIF3A*, *JAK2*, *SH2B3*, *VHL* (Coimbra, Portugal).

The NGS panel covers all the exons, intron/exon junctions (minimum 25 base pairs of the intronic sequences) and partial sequences of 5' and 3'UTR (size depending on the gene, detailed sequences and bed files available upon request.

In silico analysis:

EPAS1 genetic variants were analyzed with different *in silico* tools with the following website links:

MetaDome: https://stuart.radboudumc.nl/metadome/dashboard

PROVEAN: http://provean.jcvi.org/protein_batch_submit.php?species=human

MobiDetails: https://mobidetails.iurc.montp.inserm.fr/MD/genes

Droplet digital PCR

Droplet digital PCR was performed on patient's leukocytes and tumor DNA. Labelled TaqMan probe-based assays (Integrated DNA Technologies) were used: ACTGGCATCCTAT labelled with FAM fluorophore for the wild-type allele and ACTGGCACCCTATA with HEX fluorophore for the mutated allele. Sample partitioning was performed using the QX200 Droplet Generator (Bio-Rad), PCR amplification using the C1000 Thermal Cycler (Bio-Rad) and droplet reading using the Droplet Reader (QX 200), which provides absolute quantification in digital form.

Genomic DNA extraction for EPO promoter cloning

Cells cultured on a 10 cm plate were washed with PBS, collected in extraction buffer (50 mM Tris-HCl pH 8, 100 mM EDTA, 100 mM NaCl, 1% SDS) supplemented with 0.5 mg/ml Proteinase K (AxonLab, A3830.0500) and incubated overnight at 56°C. The next day, after 5 min at 1100 rpm, 6 M NaCl was added and the sample was mixed again during 5 min at 1100 rpm. After 10 min centrifugation at 14000 rpm, the liquid phase was transferred to a new tube and isopropanol was added. Samples were mixed during 2 min at 1100 rpm, centrifuged during 1 min at 14000 rpm and the pellet was washed with 70% ethanol. Finally, after 1 min centrifugation at 14000 rpm, the pellet was dried during 10 min, TE buffer (10 mM Tris-HCl pH 8, 1 mM EDTA) was added and the sample containing gDNA was incubated 2 hours at 37°C under shacking (350-400 rpm).

Full EPO promoter plasmid generation

The pGL3-5'HRE290-FullProm-3'HRE126 *EPO* promoter-driven luciferase plasmid was generated as follow: a PCR fragment of 604 bp, was amplified by gradient PCR with Phusion High-Fidelity DNA polymerase (Thermofisher, F530L) from HeLa gDNA using the sense primer containing BglII restriction site 5'-GTT GAA GAT CTC TAC TTT GCG GAA CTC AGC A-3' and the anti- sense primer containing HindIII restriction site 5'-CTA CAA GCT

TGT CCC TCA GCG ACC TGG-3‘. The PCR product was subsequently purified using the NucleoSpin Gel and PCR Clean-up kit (Macherey-Nagel, 740609.10) according to manufacturer’s instructions, digested with BglII and HindIII restriction enzymes, loaded on an agarose gel and extracted using the NucleoSpin Gel and PCR Clean- up kit. The digested PCR fragment was inserted into the destination vector (pGL3-5’HRE290-MinProm- 3’HRE126), opened with the same enzymes, using the T4 DNA Ligase (Thermofisher, EL0011). The integrity of full *EPO* promoter was assessed by Sanger sequencing with the sense RV3 primer 5'- CTA GCA AAA TAG GCT GTC C-3'.

Cell Culture

Human embryonic kidney cells (HEK293T, ATCC CRL-3216) and Human hepatocellular carcinoma cells (Hep3B, ATCC HB-8064) were maintained in Dulbecco’s Minimum Essential Media (DMEM) (Gibco, Life Technologies), containing L-Glutamine, supplemented with 10% FBS and 1% Penicillin/Streptomycin (10,000 Units/mL P; 10,000 µg/mL S; Gibco, Life Technologies). Human neuroblastoma cells (Kelly, Sigma 92110411-1VL) were maintained in Roswell Park Memorial Institute (RPMI) 1640 Medium (Gibco, Life Technologies), containing L- Glutamine, supplemented with 10% FBS and 1% Penicillin/Streptomycin. Cell lines were incubated in a humidified 5% CO_2 atmosphere (normoxia) at 37°C and were routinely subcultured after trypsinization. Hypoxic experiments were carried out at 0.2% O_2 and 5% CO_2 in a gas-controlled glove box (InvivO2 400, Ruskinn Technologies).

Protein extraction and quantification

Lysis buffer, containing 10 mM Tris HCl (pH 8), 1 mM EDTA, 400 mM NaCl, 1% NP-40 and protease inhibitors (2 µg/ml aprotinin, 4 µg/ml leupeptin, 2 µg/ml pepstatin and 1 mM PMSF) was used to lyse cells. Lysed cells were placed on a rotating arm at 4°C for 30 minutes to allow optimal performance of the lysis buffer. Finally, samples were centrifuged at 10’000g for 15 minutes and the protein-containing supernatant was collected. Protein concentrations were determined using the Bradford Dye Reagent (Chemie Brunschwig).

Immunoblotting

Extracted proteins were first separated, according to molecular weight, using sodium dodecyl sulphate polyacrylamide gel-electrophoresis (SDS-PAGE) gels, followed by electrotransfer to nitrocellulose membranes (Amersham Hybond-ECL, GE Healthcare). Equal amounts of protein and volume were loaded onto a 7.5% polyacrylamide gel for HIF-1α and HIF-2α.

Membranes were blocked in TBS-T (Tris- buffered Saline; 0.1% Tween-20), containing 5% non-fat dry milk, for 1 hour at room temperature. After blocking, the membranes were incubated overnight at 4 °C with primary antibodies (anti-HIF1α, BD Transduction Laboratories, 610958; anti-HIF2α, Bethyl, A700-003; anti-GFP, Proteintech, 50430-2-AP-150UL; anti-β-actin, Sigma, SP124). The following day, membranes were washed with TBST-T, and incubated during 1 hour with horseradish-conjugated secondary antibodies (anti-mouse IgG HRP, Sigma, GENA931-1ML, anti-rabbit IgG HRP, Sigma, GENA934-1ML). The signal was revealed using ECL Prime (Amersham, GERPN2232) on a C-DiGit® Western blot scanner (LI-COR Biosciences), and exported using Image Studio™ program (LI-COR Biosciences).

Quantification of transfected plasmids in real-time luciferase reporter assays

Cells were pelleted at the end of the real-time luciferase reporter. Total nucleic acids were extracted by using the Nucleospin RNA-XS kit without DNAse treatment (Macherey Nagel). A PCR was performed by using primers located in the HA tag sequence of the transfected vector encoding HA-HIF-2α (forward primer: CCATTGACGCAAATGGGCGG, reverse primer: GGATCCGAGGGAGGCGTAGT). No reverse transcription was performed to only quantify the transfected plasmids.

Legends of supplementary figures

Supplementary Table 1. Review of the *EPAS1* genetic variants identified in patients with erythrocytosis described in the literature. PGL, paraganglioma; PAH, pulmonary arterial hypertension, RCC, renal cell carcinoma; VUS, variant of unknown significance, Pheo, pheochromocytoma.

Supplementary Table 2. Review of the *EPAS1* genetic variants identified in tumors described in the literature. Pheo, pheochromocytoma; CNS, central nervous system, PGL, paraganglioma; PAH, pulmonary arterial hypertension, VUS, variant of unknown significance.

Supplementary Table 3. Clinical data of family members. Pos, Position; ID, Identification; >, indicates the proband; F, family; M, male; F, female; Hb, Hemoglobin in g/dL (normal=13-18 for men; 12-15 for women); Ht, Hematocrit in % (normal =40-52% for men; 37-47% for women), RBC, Red Blood Cells in million/mm3 (normal=4.2-5.7 for men, =4.2-5.2 for women), EPO, Erythropoietin in mU/mL (normal =5–25), NE, not explored, N: normal.

Supplementary Table 4. Detailed information and scores of *in silico* analysis. ACMG, American College of Medical Genetics and Genomics; BS, benign strong; BP, benign supporting; PM, pathogenic moderate; PP, pathogenic supporting; PS, pathogenic strong. The ACMG uses the following classification to describe variants identified in Mendelian disorders: Class1: benign; Class 2: likely benign; Class 3: variant of uncertain significance (VUS); Class 4: likely pathogenic; Class 5: pathogenic. Criteria used in our study are detailed below.

BP4: variant predicted as benign by all prediction software (here, when Mobidetails single and metapredictors scores <0.5),
BS1: allelic frequency too high compared to the frequency of the pathology (here, if the frequency is equal or greater than 5.10^4),
BS3 : non-deleterious impact demonstrated by a functional study of the variant,
PM1: variant located on a mutational hot-spot and/or a well established functional domain,
PM2: variant absent from population control databases,
PM5: variant causing a different amino acid change at the same position of a known pathogenic missense mutation,
PP1: variant co-segregating with the disease in several affected members of the same family,

PP3: variant predicted as deleterious by all prediction software (here, when Mobidetails single and metapredictors scores >0.7),
PP4: phenotype or specific family history in favor of the pathology associated with known mutation of the gene (here the polycythemia/paraganglioma/pheochromocytoma syndrome),
PS3: deleterious impact demonstrated by a functional study,
PS4: variant present in different unrelated patients and allelic frequency compatible with the presence and penetrance of the disease.

Supplemental Figure 1. Pedigree of families carrying *EPAS1* genetic variant.
Roman numerals indicate generations. Squares indicate men and circle women; black filling indicate the development of confirmed erythrocytosis; Arrows indicate probands; +, indicate the detection of the *EPAS1* mutation; -, indicate a wild type *EPAS1;* Chronic myelomonocytic leukemia (CMML).

Supplemental Figure 2. Detection of mosaicism. A) Detection of mosaicism by Next Generation Sequencing (NGS). The number and percentages of obtained reads by NGS for the *EPAS1* mutations are indicated in the tables. B) Detection of mosaicism by droplet digital PCR. Quantification of c.1591C>T *EPAS1* variant by digital droplet PCR (ddPCR) in patient 19. The ddPCR was performed on leukocytes and tumor DNA. HEX labelled droplets (in green) showed mutated allele and FAM labelled droplets (in blue) showed wild-type allele. The orange droplets are the double positive droplet and the grey droplets are empty droplets. The sequencing of the leukocytes showed the c.1591C>T variant at a variant allele frequency (VAF) of 1.16%. In tumor DNA the c.1591C>T variant was detected at a VAF of 60 %.

Supplemental Figure 3. Radar view obtained by *in silico* analysis using Mobidetails indicates various impact of the different variants. Radar view of mean normalized scores obtained by missense predictor tools (single predictors: SIFT, Polyphen 2 HumDiv and HumVar, and meta predictors: Fathmm, REVEL, ClinPred, Meta SVM, Meta LR, Mistic). The larger the red area, the higher the predicted deleterious effect. Red, orange and green colors indicated the final classification (from probably damaging, possibly damaging and benign respectively).

Supplemental Figure 4. Alignment of minimal, full core and generated full *EPO* promoter sequences inserted in the luciferase reporter vector. Sequences of minimal (MinProm), full

(FullProm) and generated full (GenFullProm) *EPO* promoter are displayed with GeneDoc 2.7. Homologous regions are highlighted in light and dark grey, respectively between full and generated construct or between all three sequences. The length for each sequence is indicated. Transcription start codon is underlined. Positions related to the coding sequence (c.) are indicated.

Supplemental Figure 5. Reporter gene assays demonstrate increased *EPO* promoter-driven luciferase activity with full *EPO* promoter compared to minimal construct. (A) End point luciferase assay was performed in HEK293 cells transfected with *EPO* minimal or full promoter constructs alone and HIF-1α or HIF-2α isoform expression plasmids. Luciferase activity is reported as the induction compared to the control (Ctrl) under hypoxic condition and represents the ratio of firefly (FF) to *Renilla* (RL) relative light units (R.L.U.). Each column represents the mean ± SEM of four to fourteen different experiments performed in duplicate. One-way ANOVA (*$p \leq 0.05$; **$p \leq 0.01$; ****$p \leq 0.0001$). (B) Immunoblots of HIF-1α and HIF-2α performed on HEK293 cells transfected with YFP-HIF-1α or YFP-HIF-2α isoform expression plasmids. Levels of expression were assessed with respectively anti-HIF-1α and HIF-2α antibodies or with an anti-GFP antibody. Actin was used as loading control. (C) End point luciferase assay was performed in different cell lines, HEK293, Hep3B and Kelly, transfected with the full *EPO* promoter. The induction was assessed under normoxic and hypoxic conditions (0.2% O_2). Luciferase activity is reported as the induction compared to the control (Ctrl) under normoxic condition and represents the ratio of firefly (FF) to *Renilla* (RL) relative light units (R.L.U.). Each column represents the mean ± SEM of four different experiments performed in duplicate.

Supplemental Figure 6. P531S HIF-2α mutant displays a significantly higher *EPO* promoter-driven luciferase activity with full promoter under normoxic and hypoxic conditions. HEK293 cells (A) and Hep3B cells (B) were transfected with 5'HRE and 3'HRE *EPO* full promoter construct and different HIF-2α mutants identified from patients, as well as with wild-type (WT) and positive P531A HIF-2α constructs, as indicated. Luciferase activity is reported as the induction compared to the control (Ctrl) under hypoxic conditions and represents the ratio of firefly (FF) to *Renilla* (RL) relative light units (R.L.U.). Each column represents the mean ± SEM of three to four different experiments performed in duplicate. One-way ANOVA, compared to HIF-2α wt in hypoxia (*$p \leq 0.05$; **$p \leq 0.01$; ***$p \leq 0.001$; ****$p \leq 0.0001$).

Supplemental Figure 7. P531S HIF-2α mutant exhibits increased *EPO* promoter-driven luciferase activity in Kelly cells. Kelly cells were transfected with 5'HRE and 3'HRE *EPO* full promoter construct and different HIF-2α mutants identified from patients, as well as with wild-type (WT) and positive P531A HIF-2α constructs, as indicated. Luciferase activity is reported as the induction compared to the control (Ctrl) under normoxic (A) or hypoxic (B) condition and represents the ratio of firefly (FF) to *Renilla* (RL) relative light units (R.L.U.). Each column represents the mean ± SEM of three different experiments performed in duplicate. One-way ANOVA, compared to HIF-2α wt (*$p \leq 0.05$; **$p \leq 0.01$).

References of Supplementary Table 1

1. Oliveira JL, Coon LM, Frederick LA, et al. Genotype–phenotype correlation of hereditary erythrocytosis mutations, a single center experience. American Journal of Hematology 2018;93(8):1029–1041.

2. Dwight T, Kim E, Bastard K, et al. Functional significance of germline EPAS1 variants. Endocr Relat Cancer 2020;28(2):97–109.

3. Lorenzo FR, Yang C, Ng Tang Fui M, et al. A novel EPAS1/HIF2A germline mutation in a congenital polycythemia with paraganglioma. J Mol Med (Berl) [Epub ahead of print].

4. Welander J, Andreasson A, Brauckhoff M, et al. Frequent EPAS1/HIF2α exons 9 and 12 mutations in non-familial pheochromocytoma. Endocr Relat Cancer 2014;21(3):495–504.

5. Schelker RC, Herr W, Grassinger J. A new exon 12 mutation in the EPAS1 gene possibly associated with erythrocytosis. Eur J Haematol 2019;103(1):64–66.

6. Camps C, Petousi N, Bento C, et al. Gene panel sequencing improves the diagnostic work-up of patients with idiopathic erythrocytosis and identifies new mutations. Haematologica 2016;101(11):1306–1318.

7. Perrotta S, Stiehl DP, Punzo F, et al. Congenital erythrocytosis associated with gain-of-function HIF2A gene mutations and erythropoietin levels in the normal range. Haematologica 2013;98(10):1624–1632.

8. Furlow PW, Percy MJ, Sutherland S, et al. Erythrocytosis-associated HIF-2alpha mutations demonstrate a critical role for residues C-terminal to the hydroxylacceptor proline. J Biol Chem 2009;284(14):9050–8.

9. Percy MJ, Beer PA, Campbell G, et al. Novel exon 12 mutations in the HIF2A gene associated with erythrocytosis. Blood 2008;111(11):5400–2.

10. Gordeuk VR, Miasnikova GY, Sergueeva AI, et al. Thrombotic risk in congenital erythrocytosis due to up-regulated hypoxia sensing is not associated with elevated hematocrit. Haematologica 2020;105(3):e87–e90.

11. Percy MJ, Chung YJ, Harrison C, et al. Two new mutations in the HIF2A gene associated with erythrocytosis. Am J Hematol 2012;87(4):439–42.

12. Alaikov T, Ivanova M, Shivarov V. EPAS1 p.M535T mutation in a Bulgarian family with congenital erythrocytosis. Hematology 2016;21(10):619–622.

13. Martini M, Teofili L, Cenci T, et al. A novel heterozygous HIF2AM535I mutation reinforces the role of oxygen sensing pathway disturbances in the pathogenesis of familial erythrocytosis. Haematologica 2008;93(7):1068–71.

14. Gale DP, Harten SK, Reid CD, Tuddenham EG, Maxwell PH. Autosomal dominant erythrocytosis and pulmonary arterial hypertension associated with an activating HIF2 alpha mutation. Blood 2008;112(3):919–21.

15. Liu Q, Tong D, Liu G, et al. HIF2A germline-mutation-induced polycythemia in a patient with VHL-associated renal-cell carcinoma. Cancer Biol Ther 2017;18(12):944–947.

16. Percy MJ, Furlow PW, Lucas GS, et al. A gain-of-function mutation in the HIF2A gene in familial erythrocytosis. N Engl J Med 2008;358(2):162–8.

17. Anžej Doma S, Kristan A, Debeljak N, Preložnik Zupan I. Congenital erythrocytosis - A condition behind recurrent thromboses: A case report and literature review. Clin Hemorheol Microcirc 2021;79(3):417–421.

18. Kristan A, Pajič T, Maver A, et al. Identification of Variants Associated With Rare Hematological Disorder Erythrocytosis Using Targeted Next-Generation Sequencing Analysis. Front Genet 2021;12689868.

19. Chandrasekhar C, Pasupuleti SK, Sarma PVGK. Novel mutations in the EPO-R, VHL and EPAS1 genes in the Congenital Erythrocytosis patients. Blood Cells Mol Dis 2020;85102479.

20. van Wijk R, Sutherland S, Van Wesel AC, et al. Erythrocytosis associated with a novel missense mutation in the HIF2A gene. Haematologica 2010;95(5):829–32.

21. Echambadi Loganathan S, Kattaru S, Chandrasekhar C, Vengamma B, Sarma PVGK. Novel mutations in EPO-R and oxygen-dependent degradation (ODD) domain of EPAS1 genes-a causative reason for Congenital Erythrocytosis. Eur J Med Genet 2022;104493.

22. Yu J, Shi X, Yang C, et al. A novel germline gain-of-function HIF2A mutation in hepatocellular carcinoma with polycythemia. Aging (Albany NY) 2020;12(7):5781–5791.

23. Mallik N, Sharma P, Kaur Hira J, et al. Genetic basis of unexplained erythrocytosis in Indian patients. Eur J Haematol 2019;103(2):124–130.

24. Comino-Mendez I, de Cubas AA, Bernal C, et al. Tumoral EPAS1 (HIF2A) mutations explain sporadic pheochromocytoma and paraganglioma in the absence of erythrocytosis. Hum Mol Genet 2013;22(11):2169–76.

25. Cakmak HM, Kartal O, Kocaaga A, Bildirici Y. Diagnosis and genetic analysis of polycythemia in children and a novel EPAS1 gene mutation. Pediatrics & Neonatology [Epub ahead of print].

26. Toledo RA, Qin Y, Srikantan S, et al. In vivo and in vitro oncogenic effects of HIF2A mutations in pheochromocytomas and paragangliomas. Endocr Relat Cancer 2013;20(3):349–59.

27. Taïeb D, Barlier A, Yang C, et al. Somatic gain-of-function HIF2A mutations in sporadic central nervous system hemangioblastomas. J Neurooncol 2016;126(3):473–481.

28. Zhuang Z, Yang C, Ryska A, et al. HIF2A gain-of-function mutations detected in duodenal gangliocytic paraganglioma. Endocrine-Related Cancer 2016;23(5):L13–L16.

29. Pacak K, Jochmanova I, Prodanov T, et al. New syndrome of paraganglioma and somatostatinoma associated with polycythemia. J Clin Oncol 2013;31(13):1690–1698.

30. Yang C, Sun MG, Matro J, et al. Novel HIF2A mutations disrupt oxygen sensing, leading to polycythemia, paragangliomas, and somatostatinomas. Blood 2013;121(13):2563–2566.

31. Buffet A, Smati S, Mansuy L, et al. Mosaicism in HIF2A-related polycythemia-paraganglioma syndrome. J Clin Endocrinol Metab 2014;99(2):E369-373.

32. Pacak K, Chew EY, Pappo AS, et al. Ocular Manifestations of Hypoxia-Inducible Factor-2α Paraganglioma-Somatostatinoma-Polycythemia Syndrome. Ophthalmology 2014;121(11):2291–2293.

33. Zhuang Z, Yang C, Lorenzo F, et al. Somatic HIF2A gain-of-function mutations in paraganglioma with polycythemia. N Engl J Med 2012;367(10):922–30.

34. Yang C, Hong CS, Prchal JT, Balint MT, Pacak K, Zhuang Z. Somatic mosaicism of EPAS1 mutations in the syndrome of paraganglioma and somatostatinoma associated with polycythemia. Hum Genome Var 2015;215053.

35. Vaidya A, Flores SK, Cheng Z-M, et al. EPAS1 Mutations and Paragangliomas in Cyanotic Congenital Heart Disease. N Engl J Med 2018;378(13):1259–1261.

36. Taïeb D, Yang C, Delenne B, et al. First report of bilateral pheochromocytoma in the clinical spectrum of HIF2A-related polycythemia-paraganglioma syndrome. J Clin Endocrinol Metab 2013;98(5):E908-913.

37. Toyoda H, Hirayama J, Sugimoto Y, et al. Polycythemia and paraganglioma with a novel somatic HIF2A mutation in a male. Pediatrics 2014;133(6):e1787-1791.

38. Favier J, Buffet A, Gimenez-Roqueplo AP. HIF2A mutations in paraganglioma with polycythemia. N Engl J Med 2012;367(22):2161; author reply 2161-2.

39. Därr R, Nambuba J, Del Rivero J, et al. Novel insights into the polycythemia-paraganglioma-somatostatinoma syndrome. Endocr Relat Cancer 2016;23(12):899–908.

40. Abdallah A, Pappo A, Reiss U, et al. Clinical manifestations of Pacak-Zhuang syndrome in a male pediatric patient. Pediatric Blood & Cancer 2020;67(4):e28096.

Supplementary Table 1 : Germline mutations and genetic variants described in the literature

Exon	Nucleotide	Protein	Phenotype	Reference	Ref
/	c.1555-121C>T	/	VUS , Erythrocytosis	Oliveira et al., 2018	1
/	c.1555-9T>C	/	VUS , Erythrocytosis	Oliveira et al., 2018	1
1	c.47delAGG	p.del17E	Erythrocytosis	Camps et al., 2016	1
6	c.739C>A	p.Arg247Ser	Found germline in patient with Pheo/PGL	Dwight et al., 2020	2
9	c.1121T>A	p.Phe374Tyr	Found germline in patient with Pheo/PGL	Dwight et al., 2020	2
9	c.1121T>A	p.Phe374Tyr	Erythrocytosis + paraganglioma	Lorenzo et al., 2012	3
9	c.1121T>A	p.Phe374Tyr	Erythrocytosis	Oliveira et al., 2018	1
9	c.1121T>A	p.Phe374Tyr	Pheochromocytoma	Welander et al., 2014	4
9	c.1157G>A	p.Ser386Asn	VUS	Oliveira et al., 2018	1
9	c.1234T>A	p.Ile412Asn	Pheochromocytoma (+ somatic Y532C)	Welander et al., 2014	4
12	c.1573G>C	p.Asp525His	Erythrocytosis	Schelker et al., 2019	5
12	c.1594T>C	p.Tyr532His	Erythrocytosis	Camps et al., 2016	6
12	c.1597A>G	p.Ile533Val	Erythrocytosis	Perrotta et al., 2013	7
12	c.1601C>T	p.Pro534Leu	Erythrocytosis	Furlow et al., 2009	8
12	c.1601C>G	p.Pro534Arg	Erythrocytosis	Oliveira et al., 2018	1
12	c.1603A>T	p.Met535Leu	Erythrocytosis	Oliveira et al., 2018	1
12	c.1603A>G	p.Met535Val	Erythrocytosis	Percy et al., Blood 2008	9
12	c.1603A>G	p.Met535Val	Erythrocytosis + thrombotic complications	Gordeuk et al., 2020	10
12	c.1604T>C	p.Met535Thr	Erythrocytosis	Oliveira et al., 2018	1
12	c.1604T>C	p.Met535Thr	Erythrocytosis	Percy et al., 2012	11
12	c.1604T>C	p.Met535Thr	Erythrocytosis	Alaikov et al., 2016	12
12	c.1605G>A	p.Met535Ile	Erythrocytosis	Martini et al., 2008	13
12	c.1609G>A	p.Gly537Arg	Erythrocytosis (3 families)	Percy et al., Blood 2008	9
12	c.1609G>A	p.Gly537Arg	Erythrocytosis	Perrotta et al., 2013	7
12	c.1609G>A	p.Gly537Arg	Erythrocytosis + PAH	Gale et al., 2008	14
12	c.1609G>A	p.Gly537Arg	Erythrocytosis + PAH	Camps et al., 2016	6
12	c.1609G>A	p.Gly537Arg	Erythrocytosis + RCC	Liu et al., 2017	15
12	c.1609G>T	p.Gly537Trp	Erythrocytosis + venous thrombosis	Percy et al., NEJM 2008	16
12	c.1609G>T	p.Gly537Trp	Erythrocytosis + pulmonary embolism + venous thrombosis + PAH	Doma et al., 2021	17
12	c.1609G>C	p.Gly537Arg	Erythrocytosis, cerebrovascular accident	Oliveira et al., 2018	1
12	c.1609G>C	p.Gly537Arg	Erythrocytosis, thrombocytopenia	Oliveira et al., 2018	1
12	c.1609G>C	p.Gly537Arg	Erythrocytosis	Kristan et al., 2021	18
12	c.1609G>A, c.1657dup	p.Gly537Arg, p.Ala553Glyfs*58	Erythrocytosis	Chandrasekhar et al., 2020	19
12	c.1615G>A	p.Asp539Asn	Erythrocytosis	Oliveira et al., 2018	1
12	c.1617C>G	p.Asp539Glu	Erythrocytosis	van Wijk et al., 2010	20
12	c.1620C>G	p.Phe540Leu	Erythrocytosis	Percy et al.,2012	11
12	c.1620C>A	p.Phe540Leu	Erythrocytosis	Oliveira et al., 2018	1
12	c.1631C>G	p.Pro544Arg	Erythrocytosis	Oliveira et al., 2018	1
12	c.1634T>C	p.Ile545Thr	VUS, Erythrocytosis	Loganathan et al., 2022	21
12	c.1645G>A	p.Glu549Lys	Erythrocytosis + Hepatocarcinoma	Yu et al., 2020	22
12	c.1650G>A	p.Arg550Gln	VUS, Erythrocytosis	Mallik et al., 2019	23
12	c.1694G>T	p.Ser565Ile	VUS, Erythrocytosis	Loganathan et al., 2022	21
12	c.1700T>C	p.Met567Thr	Found germline in sporadic case of Pheochromocytoma, classified as not causal	Comino Mendez et al., 2013	24
12	c.1715A>G	p.Gln572Arg	VUS, Erythrocytosis	Loganathan et al., 2022	21
12	c.1771C>G	p.Gln591Glu	VUS, Erythrocytosis	Loganathan et al., 2022	21
12	c.1859G>A	p.Cys620Tyr	VUS, Erythrocytosis	Loganathan et al., 2022	21
12	c.1891A>G	p.Met631Val	VUS, Erythrocytosis	Oliveira et al., 2018	1
12	c.1925A>G	p.Asp642Gly	VUS, Erythrocytosis	Oliveira et al., 2018	1
12	c.1969C>T	p.Gln657*	VUS, Erythrocytosis	Loganathan et al., 2022	21
13	c.2089C>G	p. Pro697Ala	Erythrocytosis	Cakmak et al., 2022	25
15	c.2365A>G	p.Pro785Thr	Found germline in patient with Pheo/PGL	Dwight et al., 2020	2
15	c.2465T>C	p.Met822Thr	Erythrocytosis	Camps et al., 2016	6

Supplementary Table 2 : Somatic and mosaic mutations described in the literature

Exon	Nucleotide	Protein	Phenotype	Reference	Ref	Mosaic
2	c.212C>A	p.Ser71Tyr	Pheo	Toledo et al., 2013	26	?
9	c.1104G>A	p.Met368Ile	Pheo	Welander et al., 2014	4	?
9	c.1121T>A	p.Phe374Tyr	CNS hemangioblastoma	Taieb et al., 2016	27	
12	c.1556C>T	p.Thr519Met	Periampullar Gangliocytic PGL	Zhuang et al., 2016	28	
12	c.1586T>C	p.Leu529Pro	Erythrocytosis + Pheo/PGL/Somatostatinoma syndrome + eyes lesions	Pacak et al., 2013 and Yang et al., 2013	29,30	No
12	c.1586T>C	p.Leu529Pro	Erythrocytosis + PGL + Pheo + Somatostatinoma	Buffet et al., 2014	31	Yes
12	c.1588G>A	p.Ala530Thr	Erythrocytosis + Pheo/PGL +/- Somatostatinoma syndrome + eyes lesions	Zhuang et al., 2012 and Pacak et al., 2013, 2014, Yang et al., 2015	29,32–34	Yes
12	c.1588G>A	p.Ala530Thr	Erythrocytosis + Pheo + PGL	Comino Mendez et al., 2013	24	?
12	c.1588G>C	p.Ala530Pro	Pheo + cyanotic heart disease	Vaidya et al., 2018	35	
12	c.1589C>T	p.Ala530Val	Erythrocytosis + Pheo/PGL +/- Somatostatinoma syndrome + eyes lesions	Pacak et al., 2013, Zhuang et al., 2012, Taieb et al., 2013	29,33,36	Yes
12	c.1589C>T	p.Ala530Val	Pheo + PGL	Comino Mendez et al., 2013	24	
12	c.1589C>A	p.Ala530Glu	Erythrocytosis + PGL	Toyoda et al., 2014	37	
12	c.1589C>A	p.Ala530Glu	Pheo	Welander et al., 2014	4	
12	c.1591C>T	p.Pro531Ser	PGL	Favier et al., 2012	38	
12	c.1591C>T	p.Pro531Ser	PGL	Toledo et al., 2013	26	?
12	c.1591C>T	p.Pro531Ser	Erythrocytosis+ Pheo + PGL	Comino Mendez et al., 2013	24	
12	c.1591C>T	p.Pro531Ser	Pheo	Welander et al., 2014	4	
12	c.1591C>T	p.Pro531Ser	Erythrocytosis + Pheo/PGL syndrome + eyes lesions	Darr et al., 2016	39	No
12	c.1591C>T	p.Pro531Ser	Pheo, cyanotic heart disease	Vaidya et al., 2018	35	
12	c.1591C>T	p.Pro531Ser	Erythrocytosis + PGL + Somatostatinoma + eyes lesions	Abdallah et al., 2020	40	Yes
12	c.1591C>A	p.Pro531Thr	PGL	Toledo et al., 2013	26	?
12	c.1592C>T	p.Pro531Leu	PGL	Welander et al., 2014	4	
12	c.1592C>T	p.Pro531Leu	Pheo	Toledo et al., 2013	26	?
12	c.1592C>T	p.Pro531Leu	Erythrocytosis + Pheo + PGL	Comino Mendez et al., 2013	24	
12	c.1592C>G	p.Pro531Arg	Pheo	Welander et al., 2014	4	
12	c.1592C>G	p.Pro531Arg	PGL + cyanotic heart disease	Vaidya et al., 2018	35	
12	c.1595A>G	p.Tyr532Cys	Erythrocytosis + Pheo/PGL / Somatostatinoma syndrome + eyes	Pacak et al., 2013 and Yang et al., 2013	29,30	No
12	c.1595A>G	p.Tyr532Cys	Pheo	Welander et al., 2014	4	?
12	c.1599_1604del	p.Ile533_Pro534del	Pheo	Comino Mendez et al., 2013	24	
12	c.1600_1608del	p.Pro534_Asp536del	Pheo	Comino Mendez et al., 2013	24	
12	c.1615G >T	p.Asp539Tyr	PGL	Comino Mendez et al., 2013	24	Yes
12	c.1615G>A	p.Asp539Asn	Erythrocytosis + Pheo/PGL +/- Somatostatinoma syndrome + eyes	Darr et al., 2016	39	No
12	c.1625T>C	p.Leu542Pro	Erythrocytosis + PGL	Buffet et al., 2014	31	
12	c.1630C>T	p.Pro544Ser	Periampullar Gangliocytic PGL	Zhuang et al., 2016	28	
12	c.1669 C>T	p.Gln557*	CNS hemangioblastoma	Taieb et al., 2016	27	

Supplementary Table 3 : Clinical data of the relatives

Pos cDNA	Pos prot	Family/ Patient ID	Age/Age at diagnosis	sex	Hb	Ht	RBC	EPO	Other Symptoms
c.1573G>C	**p.Asp525His**	> F13, I 1	78/63	F	19.4	56	6.53	4.9	None
		F13, II 1	53	M	20.8	58	6.49	6	None
c.1574A>G	**p.Asp525Gly**	F14/II 1	60	F	17.1	54			
		F14/II 2		M	19.4	59			
		> F14/III 1	44	M	20.5	56.9		NE	NE
		F14/III 4	/17	M					
		F14/IV 1	1.2	M	16.7	47			
		F14/IV 2	2	M	15.4	44.7	5.44		
c.1578G>C	**p.Leu526Phe**	F15/II 1	62/49	M	19.8	57.1	6.46	13.5	
		F15/II 2	60/50	F	17.5	51.4			
c.1579G>A	**p.Glu527Lys**	> F16, II 2	51	F	18.6	56.9	6.4	12.5	Congenital cataract
		F16, II 1	52	F	17.5	50			No, Tumors NE
c.1588G>T	**p.Ala530Ser**	> F17, I 1	33	M	23	68		N	None
		F17, II 1	8/6	F	16.9	49.5			No, Tumors NE
c.1597A>G	**p.Ile533Val**	F21, I 2	91	F	17.4	51.5	5.45		None
		F21, II 1	62	M	21.1	63.3	6.55		None
		> F21, III 1	32	M	20.7	58.5	6.87	15.3	No, Tumors NE
c.1604T>C	**p.Met535Thr**	F22, II 3	85/41	M	19.2/19.3	58/58	6.5/6.4		Portal vein thrombosis
		F22, III 4	53/18	M	19.5/18.8	60.1/56.8	6.76/6.33		None
		> F22 IV 2	17/6	M	18.2/15.2	52/45	5.89/5.65		None
c.1642G>A	**p.Glu548Lys**	F32, I 2	/53	M	17.2	56	5.38	17	
		F32, I 3	/51	M	18.2	55		16	
		> F32, II 1	/28	M	19.5	62	6.52	17	
c.1671G>C	**p.Gln557His**	>F33, I 1	53	M	18.2	50.7	5.68	7.4	NE
		F33, II 1	28	M	15.6	48	5		None

Supplementary Table 4 : Additional scores and details of *in silico* analysis

ID	Exon	Pos cDNA	**Pos prot**	Global gnomAD v3 Frequency	highest frequency in gnomAD v3/population	Score Radar Chart single/meta predictors, Mobidetails	PROVEAN prediction	Metadome score/ prediction	CADD Phred score	ACMG Criteria	**ACMG classification**
Patient 1	2	c.181A>G	**p.Ile61Val**	2.094e-05	0.0001963/Latino Admixed American	0.806/0.145	-0.86	0.58/ slighly intolerant	24.8		Class 3
Patient 2	6	c.587C>T	**p.Thr196Met**	7.678e-05	0.0002073/South Asian	0.837/0.439	-4.2	0.34/ intolerant	26.5		Class 3
Patient 3	6	c.734T>A	**p.Leu245Gln**	0	Variant not found	0.802/0.418	-5.37	0.71/ neutral	28.5	PM2	Class 3
Patient 4	7	c.818T>G	**p.Leu273Arg**	0.0005	0.001206/African/African American	0.830/0.467	-5.68	0.50/ intolerant	29.2	BS1, PP3	Class 3
Patient 5	9	c.1046A>G	**p.Lys349Arg**	0	Variant not found	0.446/0.255	-1.04	0.34/ intolerant	23.9	PM2, BP4	Class 3
Patient 6	9	c.1057G>C	**p.Val353Leu**	0	Variant not found	0.643/0.321	-1.66	0.38/ intolerant	23.5	PM2	Class 3
Patient 7 Patient 8 Patient 9	9	c.1121T>A	**p.Phe374Tyr**	0.0045	0.01266/Middle Eastern	0.341/0.179	-1.02	1.27/ tolerant	22.7	BS1, BP4	Class 2
Patient 10	11	c.1478A>G	**p.Asp493Gly**	0	Variant not found	0.337/0.140	-3.05	0.47/ intolerant	21	PM2, BP4	Class 3
Patient 11 Patient 12	11	c.1510C>G	**p.Leu504Val**	6.977e-06	0.00006540/Latino Admixed American	0.840/0.454	-2.14	0.58/ slighly intolerant	25.7	PS4 supporting	Class 3
Patient 13	12	c.1573G>C	**p.Asp525His**	0	Variant not found	0.897/0.878	-6.12	0.29/ intolerant	32	PM2, PP3, PM5, PS4 supporting	Class 4
Patient 14	12	c.1574A>G	**p.Asp525Gly**	0	Variant not found	0.897/0.896	-6.12	0.29/ intolerant	32	PM2, PP3, PS3, PP1 strong	Class 5
Patient 15	12	c.1578G>C	**p.Leu526Phe**	0	Variant not found	0.892/0.846	-3.36	0.25/ intolerant	25	PM2, PM1, PP3,PS3	Class 4
Patient 16	12	c.1579G>A	**p.Glu527Lys**	0	Variant not found	0.880/0.851	-3.26	0.24/ intolerant	32	PM2, PP3,PS3	Class 4
Patient 17	12	c.1588G>T	**p.Ala530Ser**	0	Variant not found	0.892/0.835	-2.52	0.2/ intolerant	28.8	PM1, PM2, PM5, PP3, PS3	Class 5
Patient 18	12	c.1589C>A	**p.Ala530Glu** 1,5% reads	0	Variant not found	0.895/0.876	-4.3	0.2/ intolerant	27	PM1, PM2, PP3, PS1, PS4 moderate	Class 5
Patient 19	12	c.1591C>T	**p.Pro531Ser** 1,9% read	0	Variant not found	0.905/0.885	-6.99	0.17/ Highly intolerant	26.4	PM2, PP3, PM1, PS1, PS3, PS4 moderate	Class 5
Patient 20	12	c.1595A>G	**p.Tyr532Cys**	0	Variant not found	0.895/0.888	-7.83	0.18/ intolerant	32	PM1, PM2, PM5, PS3, PP3, PS4 moderate	Class 5
Patient 21	12	c.1597A>G	**p.Ile533Val**	0	Variant not found	0.886/0.806	-0.87	0.11/ Highly intolerant	26.4	PM1, PM2, PP3, PS3, PS4 supporting	Class 5
Patient 22 Patient 23	12	c.1604T>C	**p.Met535Thr**	0	Variant not found	0.892/0.896	-5.25	0.07/ Highly intolerant	27.1	PM2, PP3, PS4, PM, PM1	Class 5
Patient 24	12	c.1609G>C	**p.Gly537Arg**	0	Variant not found	0.845/0.560	-2.76	0.08/ Higlhy intolerant	31	PM1, PM2, PP3, PS1, PS3	Class 5
Patient 25 Patient 26 Patient 27 Patient 28 Patient 29	12	c.1609G>A								PM1, PM2, PP3, PS, PS3, PS4	
Patient 30	12	c.1612G>A	**p.Glu538Lys**	0	Variant not found	0.872/0.789	-2.9	0.14/ Highly intolerant	32	PM2, PP3	Class 3
Patient 31	12	c.1620C>A	**p.Phe540Leu**	0	Variant not found	0.894/0.856	-5.26	0.18/ intolerant	26.1	PM2, PP3, PS4 supporting	Class 3
Patient 32	12	c.1642G>A	**p.Glu548Lys**	1.396e-05	0.00002941/European (non-Finnish)	0.864/0.573	-1.99	0.34/ intolerant	26.3	PP3	Class 3
Patient 33	12	c.1671G>C	**p.Gln557His**	6.983e-06	0.00001470/European (non-Finnish)	0.755/0.272	-1.57	0.36/ intolerant	22.8	PM2, BS3	Class 3
Patient 34	12	c.1679C>A	**p.Pro560His**	4.187e-05	0.003165/Middle Eastern	0.607/0.139	-1.71	0.37/ intolerant	17.26		Class 3
Patient 35	12	c.1685A>T	**p.His562Leu**	0	Variant not found	0.299/0.184	-1.81	0.35/ intolerant	19.19	PM2, BP4	Class 3
Patient 36 Patient 37	12	c.1700T>C	**p.Met567Thr**	0.0002	0.001435/Other 0.0009168/Latino Admixed/American	0.406/0.160	-1.23	0.35/ intolerant	22.7	BP4	Class 3
Patient 38	12	c.1705A>G	**p.Asn569Asp**	4.192e-05	0.0002076/South Asian	0.309/0.108	-0.92	0.37/ intolerant	20.9	BP4	Class 3
Patient 39	12	c.1750C>T	**p.Leu584Phe**	6.978e-06	0.00001470/European (non-Finnish)	0.233/0.091	-1.04	0.8/ Neutral	15.59	BP4	Class 3
Patient 40	12	c.1805G>A	**p.Arg602Gln**	1.397e-05	0.00002415/African/African American	0.192/0.092	-0.41	0.65/ slighly intolerant	14.79	BP4	Class3
Patient 41	12	c.1960G>A	**p.Val654Ile**	2.094e-05	0.0001309/Latino Admixed American	0.305/0.065	-0.11	0.61/ slighly intolerant	10.35	BP4	Class3
Patient 42	12	c.1973G>A	**p.Arg658His**	0.0002	0.0006280/African/African American	0.196/0.088	-0.27	0.53/ slighly intolerant	4.46	BP4	Class3
Patient 43	15	c.2474G>A	**p.Arg825Gln**	6.98e-06	0.00001470/European (non-Finnish)	0.418/0.164	-1.7	0.75/ neutral	22.9	BP4	Class 3

Supplementary Figure 1 Additional pedigree

Family 15: c.1578G>A, p.Leu526Phe

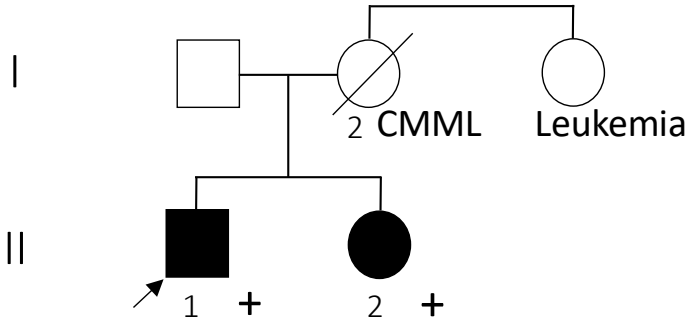

Family 21: c.1597A>G, p.Ile533Val

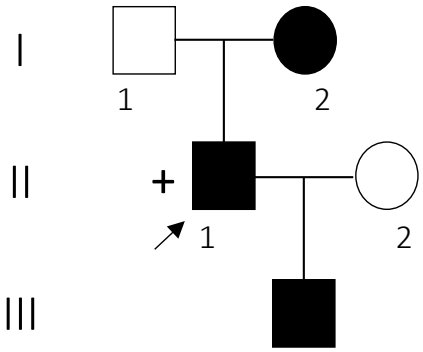

Family 16: c.1579G>A, p.Glu527Lys

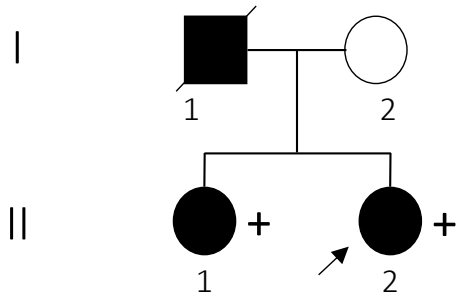

Family 20, c.1595A>G, p.Tyr532Cys

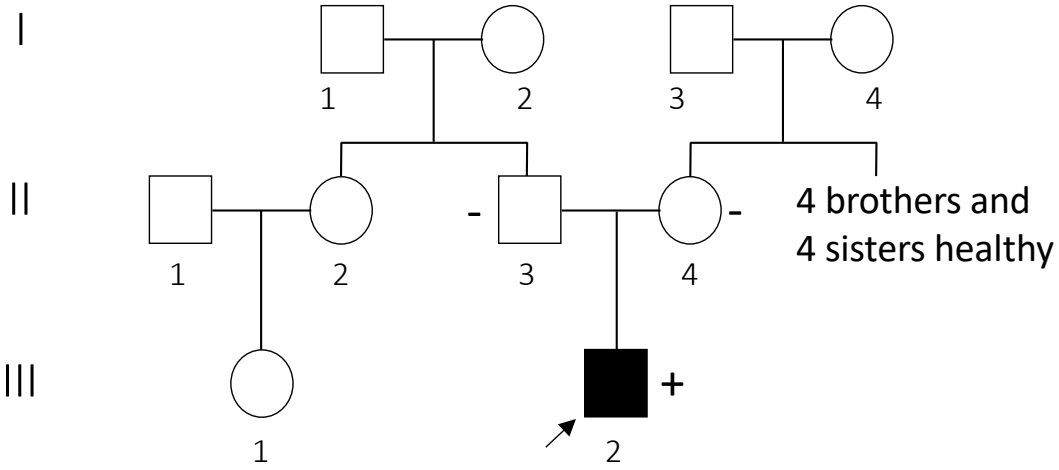

Family 27: c.1609G>A, p.Gly537Arg

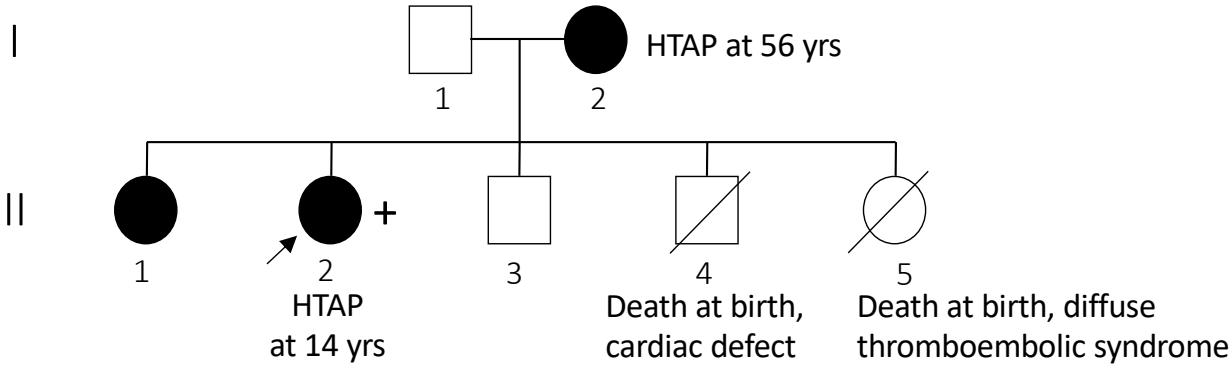

Family 30: c.1612G>A, p.Glu538Lys

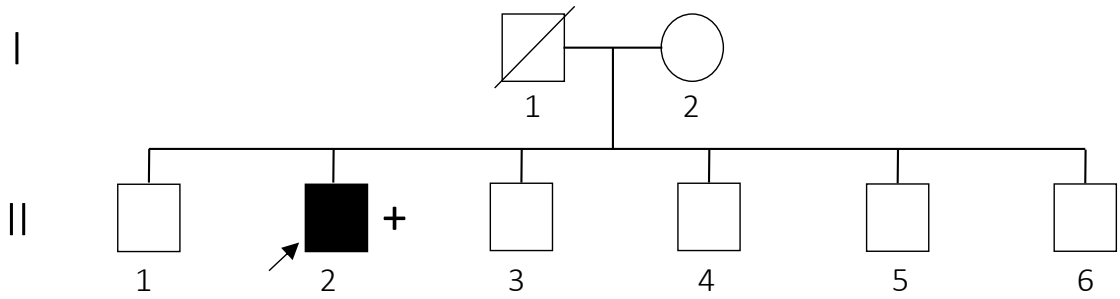

Family 32: c.1642G>A, p.Glu548Lys

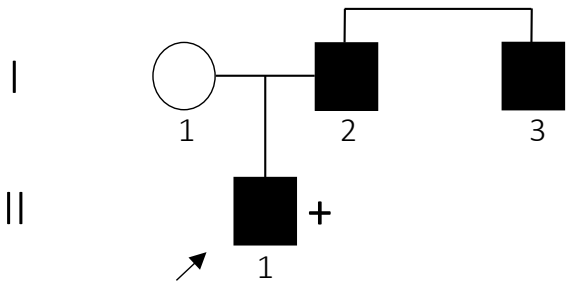

Family 33: c.1671G>C, p.Gln557His

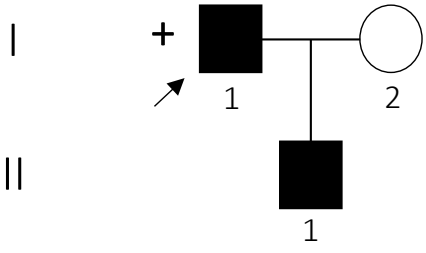

Supplementary Figure 2

A Detection of mosaicism by NGS

Patient 19: c.1589C>A, p.Ala530Glu: 1.5% of reads

n° Run	DNA sample	Sequencing Method	Variant Detection	Wild type: C	Mutated: A	Total reads	**% of mutated reads**
Run 1	1st sample	Sophia Genetics	Sophia DDM (Sophia Genetics)	2447	36	2483	**1,45**
Run 2	2nd sample	Sophia Genetics	Sophia DDM (Sophia Genetics)	2251	36	2287	**1,57**

Patient 20: c.1591C>T, p.Pro531Ser: 1.9% of reads

n° Run	DNA sample	Sequencing Method	Variant Detection	Wild type: C	Mutated: T	Total reads	**% of mutated reads**
Run 1	1st sample	Haloplex			Not detected		**/**
Run 2	1st sample	Sophia Genetics	Sophia DDM (Sophia Genetics)	4153	79	4234	**1,87**
Run 3	1st sample	Sophia Genetics	bam files loaded in Alamut	2329	19	2354	**0,81**
Run 4	2nd sample	Sophia Genetics	bam files loaded in Alamut	3669	24	3697	**0,65**

B Detection of mosaicism by Droplet Digital PCR

Control

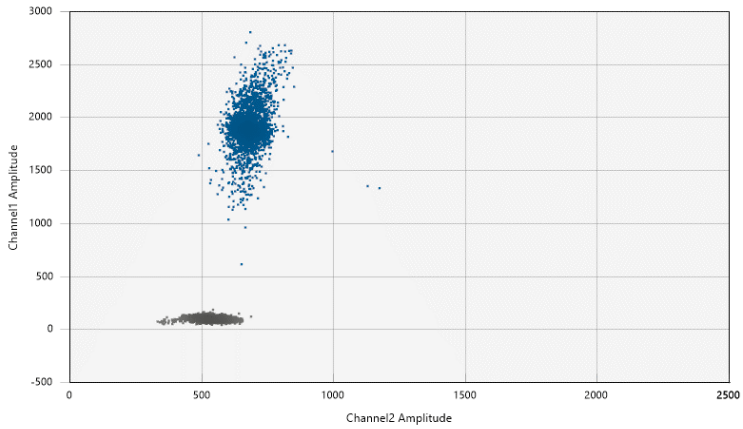

- Empty droplets
- Wild type droplets
- Mutated c.1591C>T droplets
- Wild type + c.1591C>T droplets

Leukocytes DNA

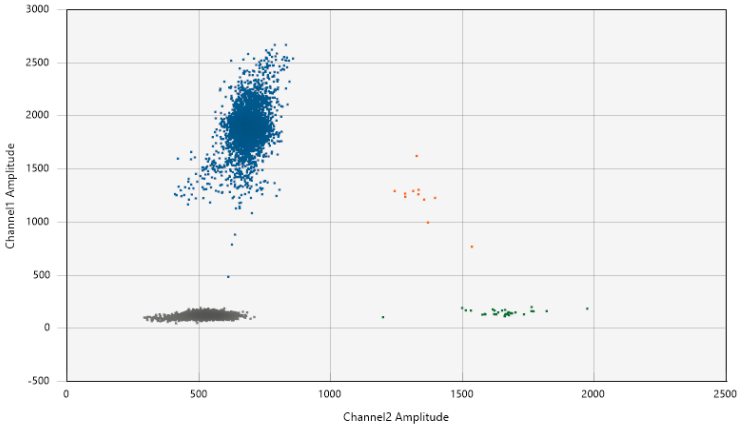

Tumor DNA

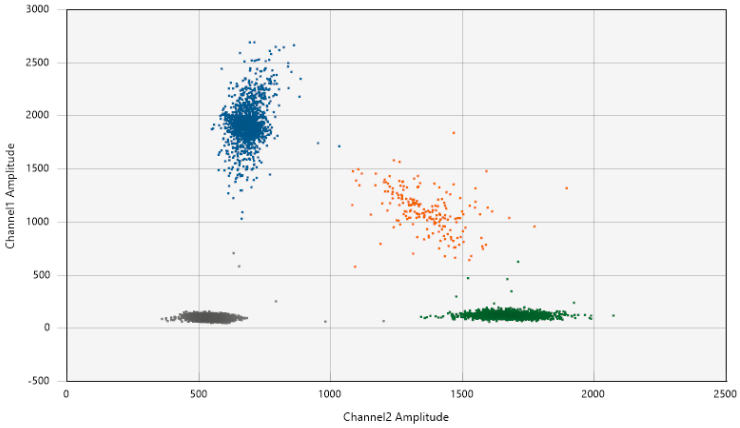

Supplementary Figure 3

In silico analysis by Mobidetails, Radar view of missense predictor

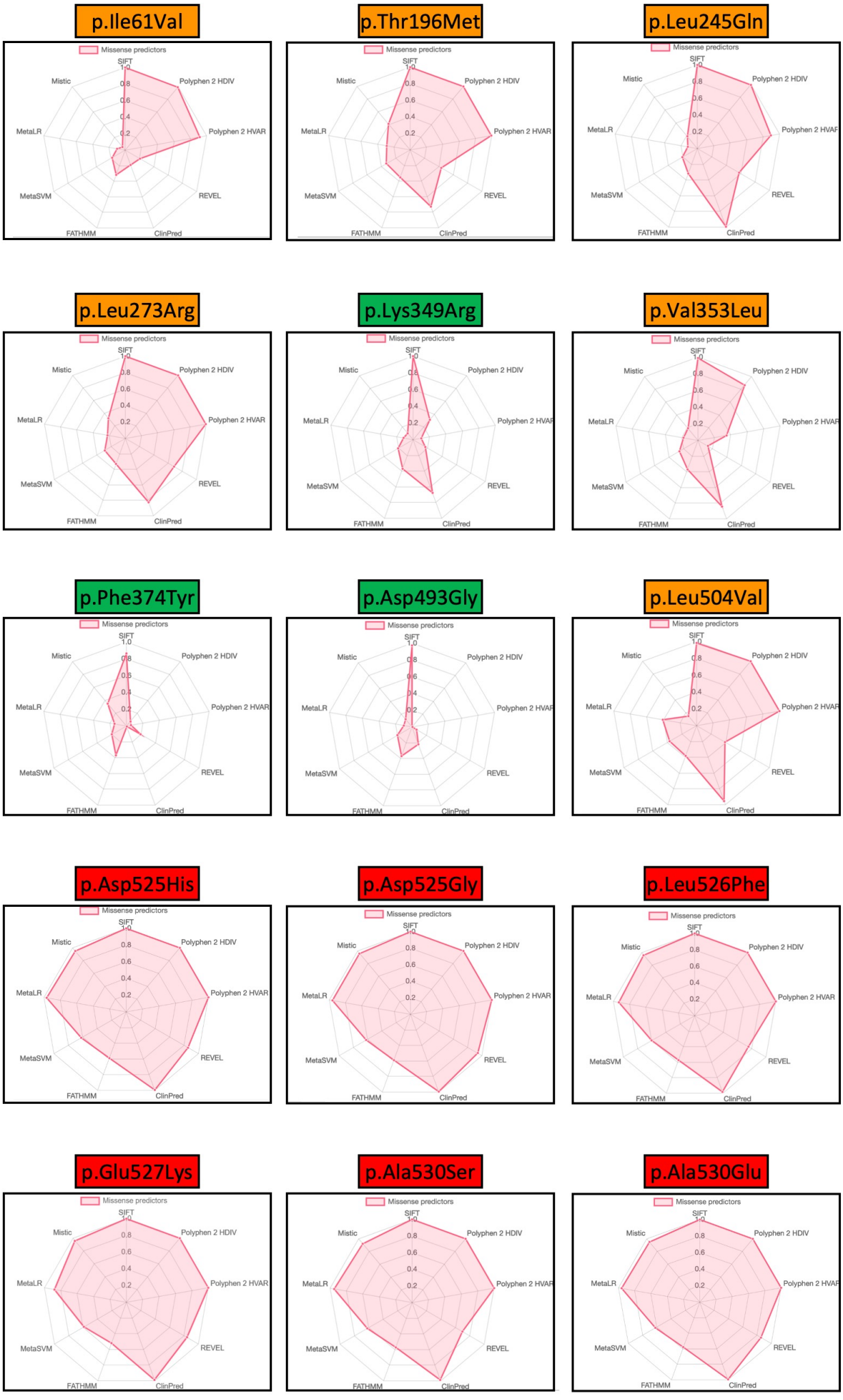

p.Pro531Ser

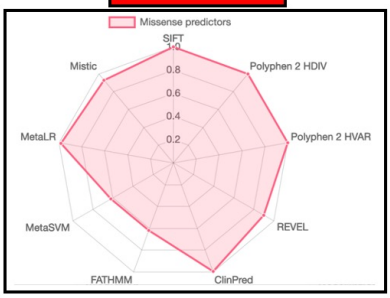

p.Tyr532Cys

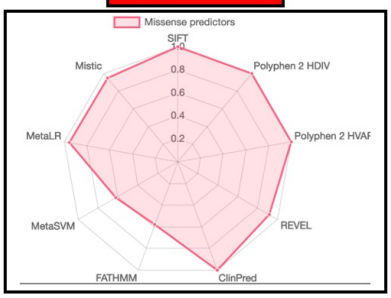

p.Ile533Val

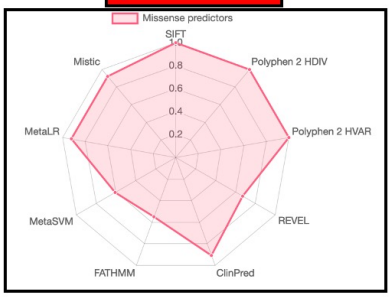

p.Met535Thr

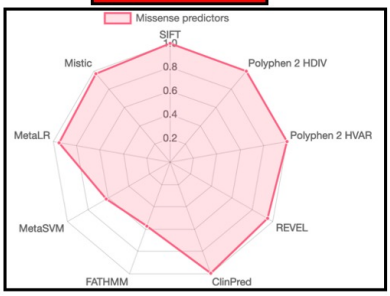

p.Gly537Arg

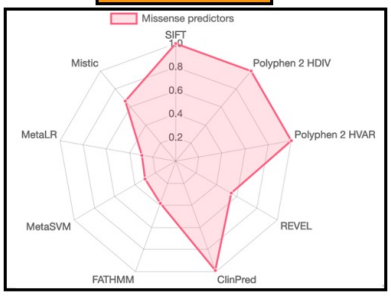

p.Glu538Lys

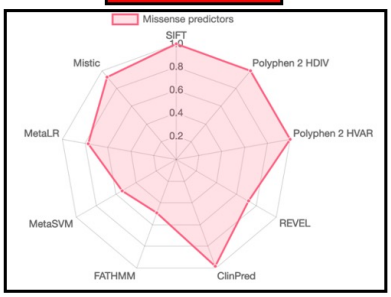

p.Phe540Leu

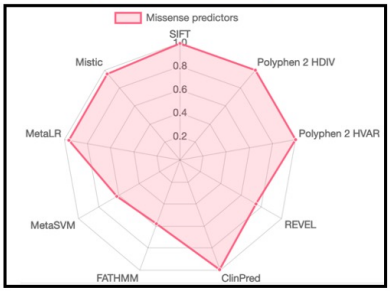

p.Glu548Lys

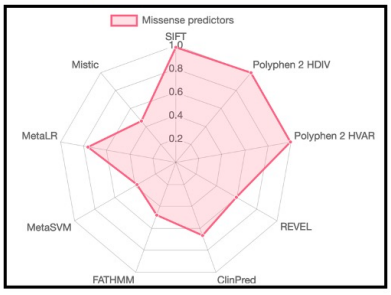

p.Gln557His

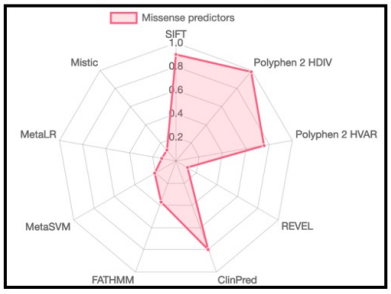

p.Pro560His

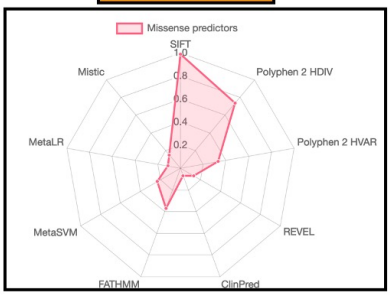

p.His562Leu

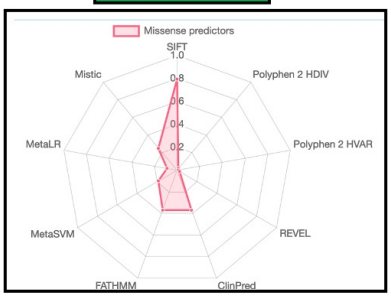

p.Met567Thr

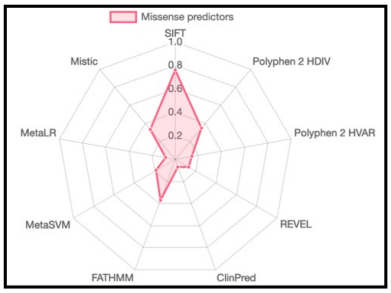

p.Asn569Asp

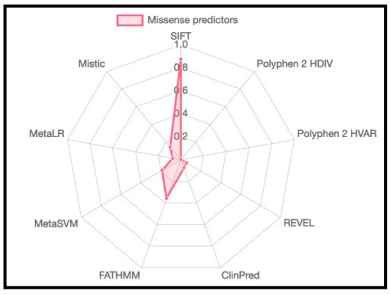

p.Leu584Phe

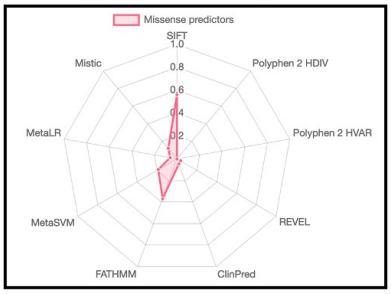

p.Arg602Gln

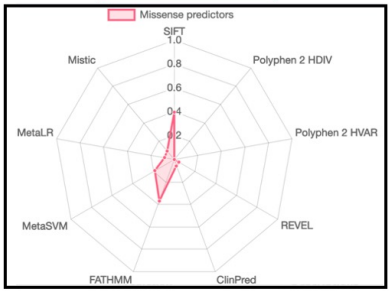

p.Val654Ile

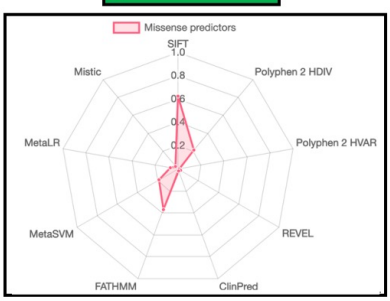

p.Arg658His

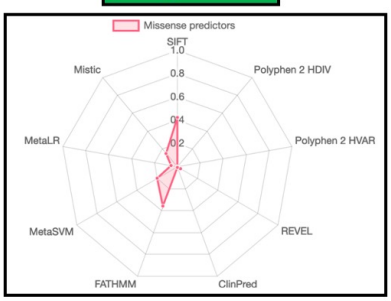

p.Arg825Gln

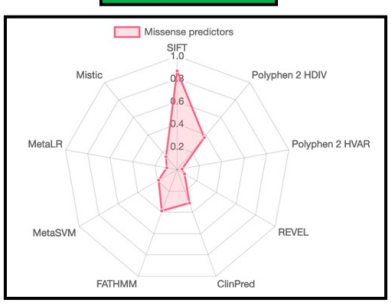

Supplementary Figure 4 Construction of *EPO*-promoter reporter vector

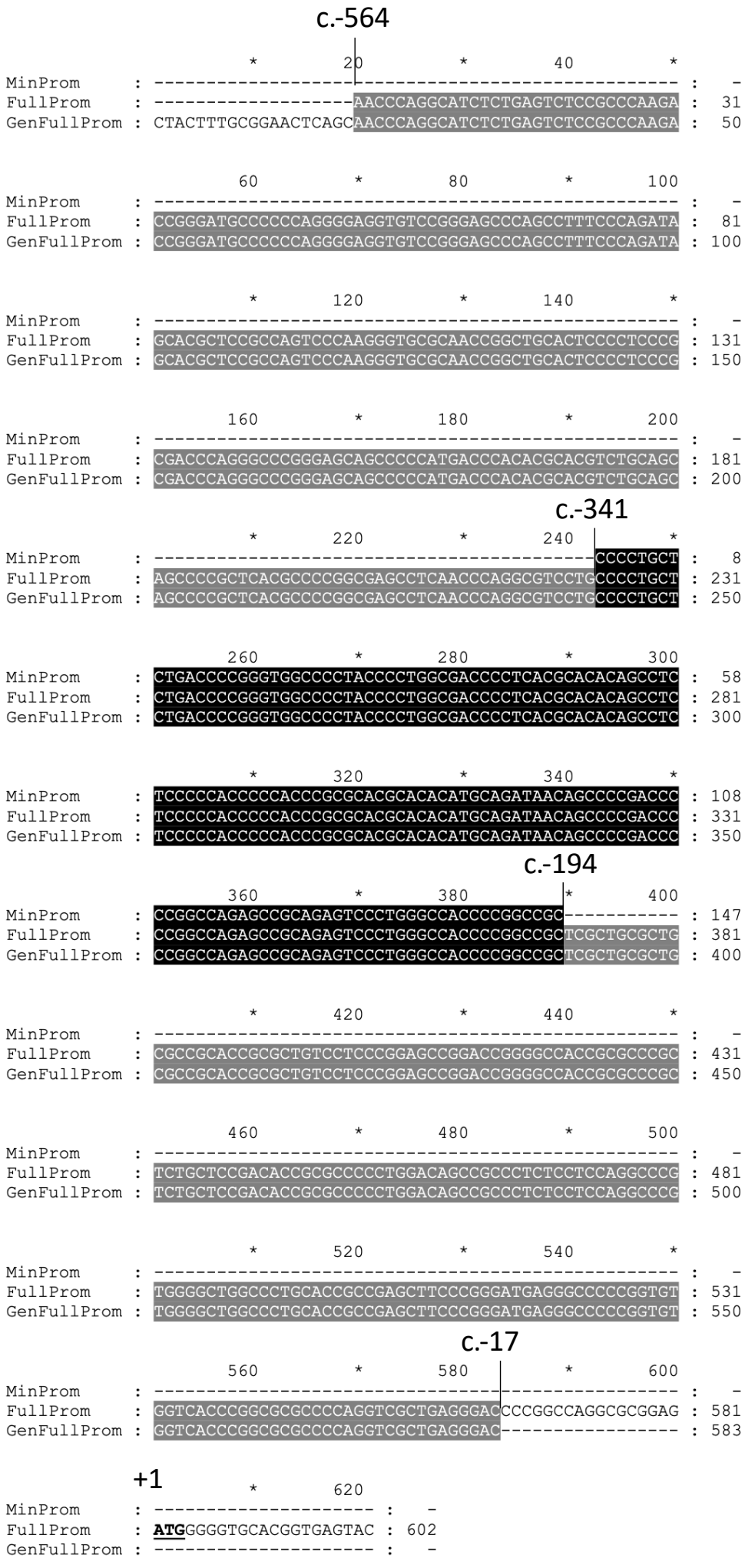

Supplementary Figure 5

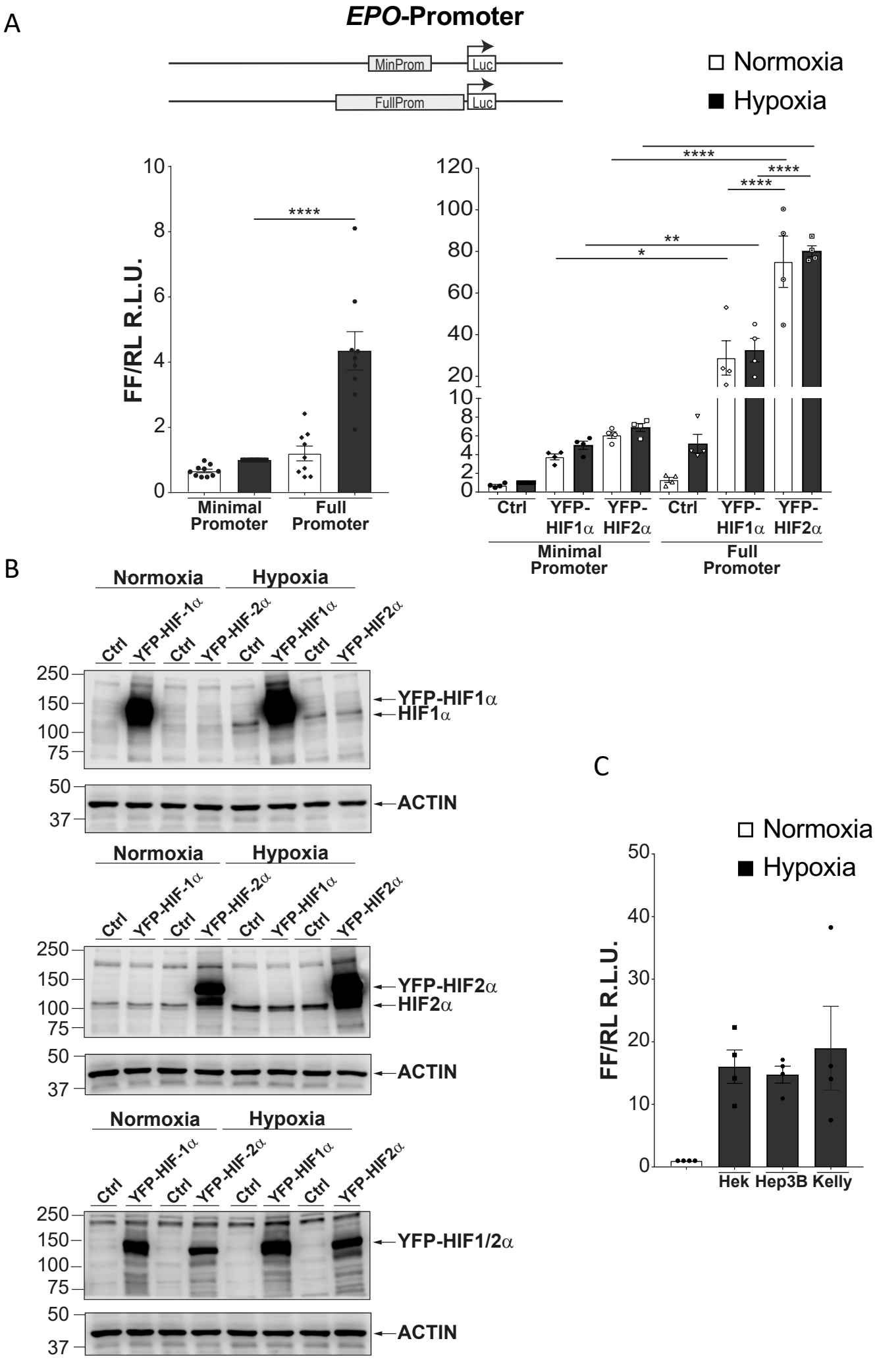

Supplementary Figure 6

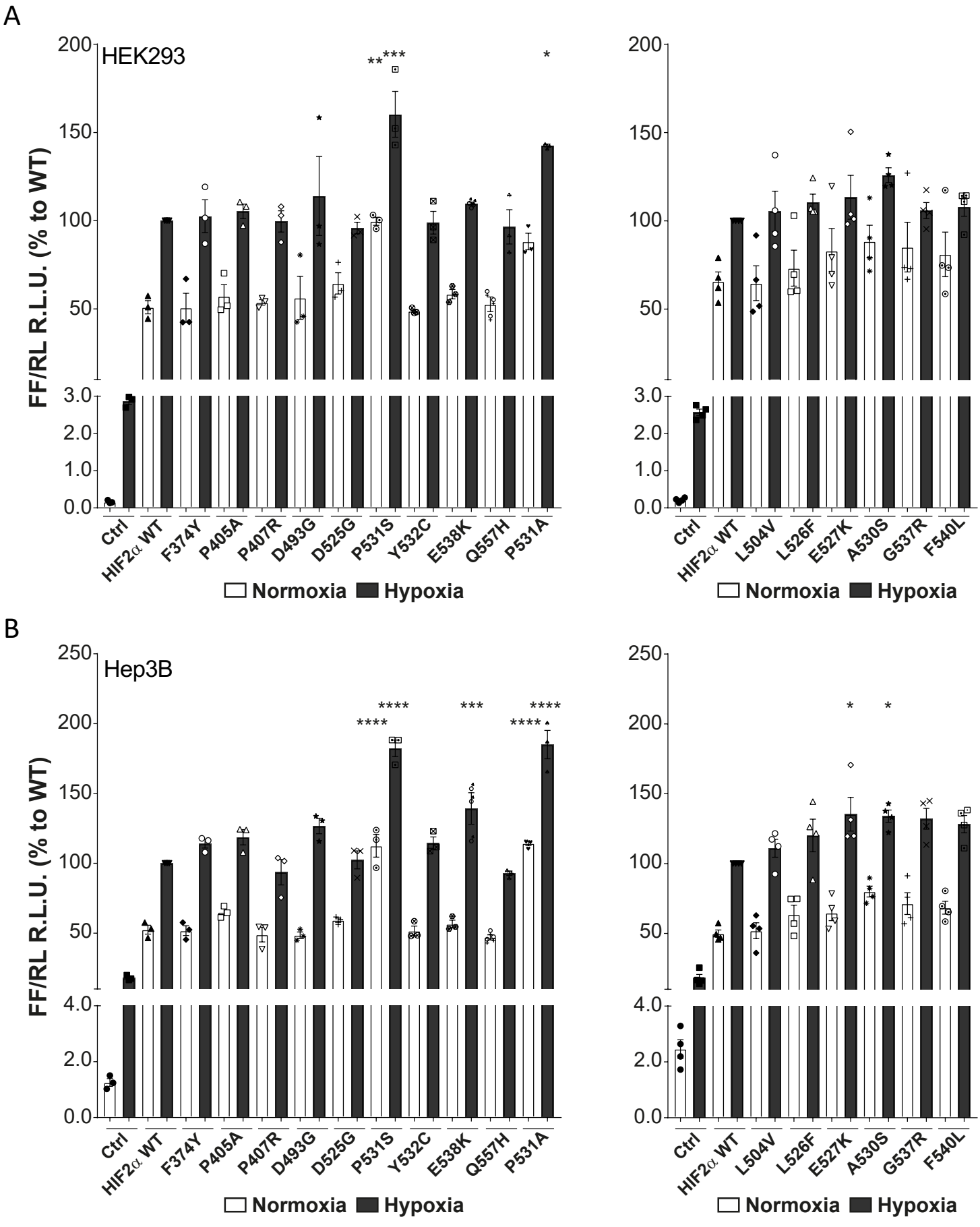

Supplementary Figure 7